2

UCRL-CR--104490-Exe.Summ.

DE90 015401

Tropospheric Nitrogen: The Influence of Anthropogenic Sources on Distributions and Deposition

Executive Summary

J.E. Penner, C.S. Atherton, J.J. Walton

This paper was prepared as a final report
to the Environmental Protection Agency under
Interagency Agreement No. DW89932676-01-1.

July 1990

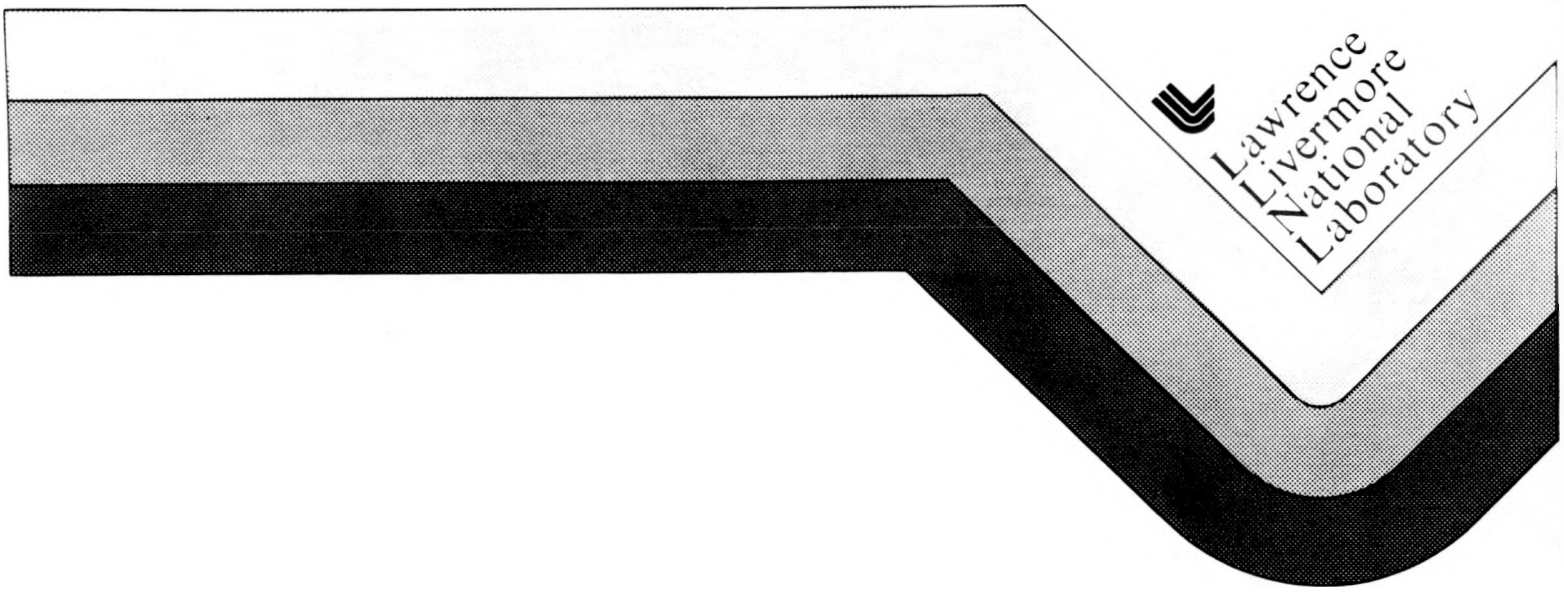

TROPOSPHERIC NITROGEN: THE INFLUENCE OF ANTHROPOGENIC SOURCES ON DISTRIBUTIONS AND DEPOSITION

Executive Summary

J.E. Penner, C.S. Atherton, J.J. Walton

Lawrence Livermore National Laboratory
Livermore, CA 94550

July 1990

TROPOSPHERIC NITROGEN: THE INFLUENCE OF ANTHROPOGENIC SOURCES ON DISTRIBUTIONS AND DEPOSITION

J.E. Penner, C.S. Atherton, J.J. Walton

Atmospheric and Geophysical Sciences Division
Lawrence Livermore National Laboratory
University of California
Livermore, CA 94550

Executive Summary

1. Introduction

Nitrogen oxides are important for global photochemistry because they determine whether O_3 is produced or destroyed. Elevated concentrations of O_3 are of concern because O_3 affects the growth of plants and the respiratory systems of man and other animals (Tilton, 1989; Reich and Amundson, 1985), because it absorbs infrared radiation and contributes to the greenhouse warming (Ramanathan et al., 1985), and because it is a key player in the photochemistry of hydroxyl, the most important chemical scavenger in the atmosphere (Logan et al., 1981; Penner, 1990). In regions of high NO_x concentrations, a photochemical sequence, initiated by the reaction of CO with OH, leads to O_3 production:

$$\begin{aligned} CO + OH &\rightarrow CO_2 + HO_2 \\ HO_2 + NO &\rightarrow NO_2 + OH \\ NO_2 + h\nu &\rightarrow NO + O \\ O + O_2 &\rightarrow O_3 \end{aligned} \qquad (1)$$

Net: $$CO + h\nu \rightarrow CO_2 + O_3 + O_2$$

At low NO_x concentrations, the second reaction listed above, the reaction of HO_2 with NO, is slow. Instead, HO_2 reacts with O_3 and the reaction sequence initiated by the reaction of CO with OH leads to O_3 destruction:

$$\begin{aligned} CO + OH &\rightarrow CO_2 + HO_2 \\ HO_2 + O_3 &\rightarrow OH + O_2 + O_2 \end{aligned} \qquad (2)$$

Net: $$CO + O_3 \rightarrow CO_2 + 2O_2.$$

If the ratio of the concentration of NO to O_3 is greater than the ratio of the reaction rate coefficients k_2/k_1 (where k_2 is the rate coefficient for the reaction of HO_2 with O_3 and

k_1 is the rate coefficient for the reaction of HO_2 with NO), the first sequence above is faster and O_3 is produced. For typical O_3 concentrations, this occurs when NO_x (=NO + NO_2) concentrations are around 20 to 50 ppt. Because observed concentrations of NO_x in ocean regions are near this limit, large portions of the atmosphere are close to values where the reaction sequence (1) may begin to dominate over reaction sequence (2) if NO_x concentrations increase. Indeed, fossil fuel emissions of NO_x have increased substantially over the last two decades (Hameed and Dignon, 1988). A further increase in these sources could fundamentally alter the atmosphere by turning vast portions from regions which are typically regions of net O_3 destruction to regions of net O_3 production.

In addition to its importance for O_3 and the photochemistry of the troposphere, reactive nitrogen is also important because NO_3^-, the end product of the reactive nitrogen cycle, is a key component of acid rain and a key nutrient for both ocean phytoplankton and for land biota.

In this paper, we describe our simulations of the global cycle of reactive nitrogen. We use a three-dimensional chemistry-transport-deposition model. Our model is a Lagrangian model in which trace species react and are carried in constant-mass air parcels; the parcels are advected by winds calculated by the NCAR Community Climate Model (CCM), a nine-layer general circulation model (Pitcher et al., 1983; Williamson, 1983). In Section 2, we describe the model, together with our specification of the reactive nitrogen sources. A comparison of our predicted concentrations and deposition amounts with measurements appears in Section 3. Section 4 describes our model results for predicted distributions, while Section 5 describes our results for deposition. Section 6 summarizes a regional analysis of sources and deposition. Our conclusions appear in Section 7.

2. Model Description

The model we use is based on the GRANTOUR model described in Walton et al. (1988). A full description of the modifications needed to describe the nitrogen cycle together with a comprehensive comparison of the model results to measurements is presented in Penner et al. (1990). Here, we outline the basic features of this model. The chemistry of reactive nitrogen in the model has been simplified. Thus, we treat reactive nitrogen as NO_x ($NO+NO_2$) and HNO_3. The ratio of NO to NO_2 is determined by the photostationary state such that the reaction of NO with O_3 is instantaneously balanced by photolysis of NO_2:

$$\begin{aligned} NO + O_3 &\rightarrow NO_2 + O_2 \\ NO_2 + h\nu &\rightarrow NO + O \quad . \end{aligned}$$

Transformations between NO_x and HNO_3 follow the reactions:

$$\begin{aligned} NO_2 + OH &\rightarrow HNO_3 \\ HNO_3 + OH &\rightarrow H_2O + NO_x + O_x \\ HNO_3 + h\nu &\rightarrow OH + NO_2. \end{aligned}$$

Here, we have assumed that NO_3 (which is produced by the reaction of HNO_3 with OH) is immediately photolized to produce either NO or NO_2. To calculate the rates of these

reactions in the model, we specify the O_3 fields based on measurements, allowing them to vary with latitude, height, and season (Wilcox and Belmont, 1977; Routhier et al., 1980; Oltmans, 1981; Kirchoff, 1984; and WMO, 1985). The concentration of hydroxyl, OH, is specified to vary with latitude and height, according to the predicted concentrations in the LLNL two-dimensional model (Wuebbles, et al., 1987). We also use photolysis rates from the LLNL model, but our reaction rate coefficients, which vary with temperature and pressure, have a longitudenal variation, as well, according to the monthly-averaged temperatures calculated in the CCM.

Dry deposition velocities are applied to the concentrations of NO, NO_2, and HNO_3 in the lowest 100 mb of the atmosphere according to:

$$\begin{aligned} v_d(NO) &= 0.05 \text{ cm/s} \\ v_d(NO_2) &= 0.25 \text{ cm/s} \\ v_d(HNO_3) &= 0.5 \text{ cm/s}, \end{aligned} \tag{3}$$

which are chosen as representative mean values (Atherton et al., 1990; Finlayson-Pitts and Pitts, 1986). Precipitation scavenging of HNO_3 is assumed to be proportional to the precipitation rate in the CCM. Thus, the rate of removal of HNO_3 from level k in the atmosphere is given by

$$R_j(k) = S_j \, P_j(k) \tag{4}$$

where S_j is assumed to be 4.8 cm^{-1} for stratoform precipitation. For convective precipitation Equation (4) is modified as discussed in Walton et al. (1988) and S_j is set at 9.4 cm^{-1}. These values for S were chosen based on an analysis of six years of data for nitrate scavenging in precipitation on Long Island (Sperber and Hameed, 1986).

The sources of reactive nitrogen in our model are specified according to Table 1. Figure 1 shows the distribution of these sources with latitude and longitude in the model. Except for the stratospheric source (which varies only with latitude), all of the sources in Table 1 are stronger over land areas. Fossil fuel is by far the largest source of NO_x, and its dominant contribution to the total of all sources is seen in the maximum contours over North America, Europe, and Japan and Eastern Asia. The biomass burning source (specified here with an annual average source function) is a major contributor in the tropics and Southern Hemisphere, while soil microbial sources shift in importance from the Southern Hemisphere in January to the Northern Hemisphere in July, according to source rates that are set to zero in deserts and for sub-freezing temperatures and take on values that are approximately one half the average emission factors given for a Colorado grassland and a tropical forest soil by Williams et al. (1987) and Kaplan et al. (1988), respectively. Though very large relative to other sources, the contribution of anthropogenic sources to NO_x concentrations in remote areas has, until recently, been considered negligible due to the relatively short lifetime (a few days) for conversion of NO_x to HNO_3 followed by rainout and deposition of HNO_3. In the following, we show that these sources play a substantial role in maintaining the concentrations of NO_x and HNO_3 in remote areas.

Table 1. NO_x sources used in the model simulations.

Source	Emission Rate (Mt N/yr)	Description
Fossil-fuel combustion	22.4	The 1980 fossil-fuel source distribution given in Hameed and Dignon (1988).
Lightning discharges	3.0	The three-dimensional distribution is estimated with the procedure described by Hameed et al. (1981). NO_x produced by cloud-to-cloud lightning flashes was distributed, with a profile that is constant in density between 75 and 506 mb, while that from cloud to ground was distributed from the surface to 339 mb. The total source strength was based on the estimate of Borucki and Chamiedes (1984) and is similar to that of Hameed et al. (1981).
Soil microbial activity	10.0	Distribution on land prescribed according to land type as described in text.
Production in stratosphere	1.0	The latitudinal and vertical distribution were determined by the rate of production of odd nitrogen from the reaction of N_2O with $O(^1D)$, as determined in the LLNL 2-D transport kinetics model (Wuebbles et al., 1987).
Biomass burning	5.8	Distribution on land according to land type as described in Hao et al. (1989).

3. Comparison to Measurements

We have attempted to validate our model by comparison of the predicted concentrations and wet deposition values with measured quantities. A comparison of the measured and predicted deposition of nitrate in precipitation at a set of remote locations is given in Table 2. As shown there, the model is within a factor of two of the observations at most of these sites with some of the predictions being high and some being low relative to the measurements. As reported in Penner et al. (1990), the model also does well in predicting the removal of nitrate by precipitation in the United States, especially in summer. In Europe, the predicted rainout is too small, especially in January, perhaps because the winds in the CCM are too high and the model placement of precipitation fields is incorrect relative to the observed fields and the emissions (see Penner et al., 1990). Sensitivity tests, in which the precipitation removal coefficient S_j (Equation 4) was increased by a factor of 2, did not change the agreement, showing that essentially all of the nitrate that comes into contact

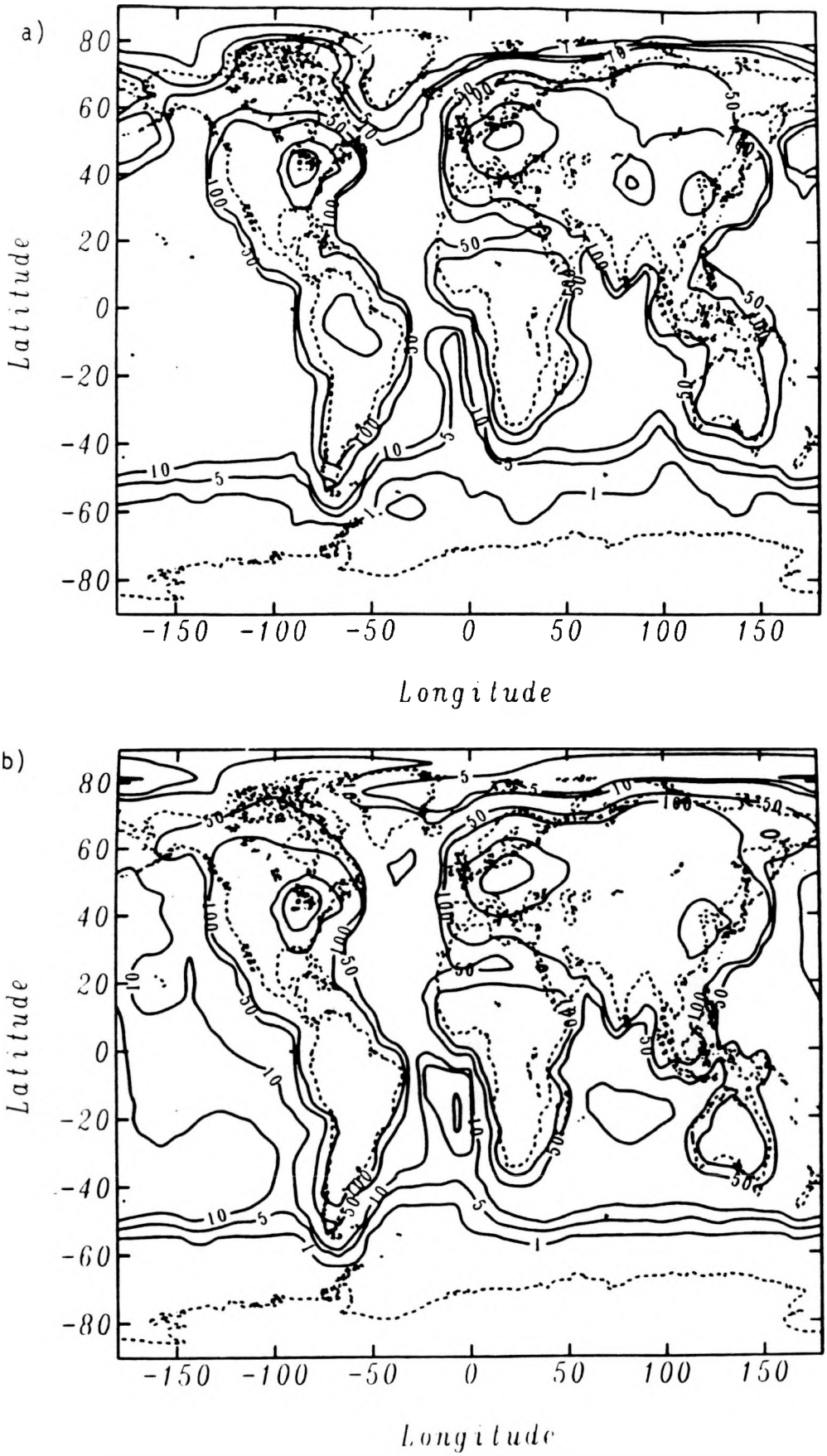

Figure 1. The distribution of the sum of all sources used in the model (see Table 1) for (a) January and (b) July. Contour intervals are 1, 5, 10, 50, 100, 500, 1000, and 1500 kg N/km^2-yr.

with a precipitation event is removed. The comparison of the predicted and observed wet deposition at remote areas shown in Table 2, confirms that, overall, the transport of nitrate to remote regions is relatively well represented.

Table 2. Comparison of measured and calculated wet deposition in μmoles/liter at remote stations.

			JANUARY		JULY		
Site	Lat.	Lon.	Data	Model	Data	Model	Reference
Point Barrow, Alaska[a]	71N	157W	–	–	0.4	2.2	Dayan et al., 1985
Poker Flat, Alaska[b]	65N	147W	–	–	2.1	1.7	Dayan et al., 1985
Denali National Park, Alaska[b]	64N	149W	2.1	2.6	2.7	1.9	Knapp et al., 1988
Adrigole, Ireland[a]	52N	10W	3.0	1.3	6.6	11.4	Keene, 1988
Mauna Loa, Hawaii[b]	20N	156W	1.1	0.5	1.1	0.7	Knapp et al., 1988
American Samoa[b]	14S	171W	0.3	0.6	0.3	0.6	Knapp et al., 1988
Katherine, Australia[c]	14S	132E	4.3	2.5	–	–	Likens et al., 1987; Keene, 1988
Amsterdam Island[c] (Indian Ocean)	38S	78E	1.7	0.5	1.2	0.9	Keene, 1988

[a]The observations represent an average of two years of data.

[b]The observations represent an average of at least three years of data.

[c]The observations represent an average of six years of data.

Figure 2 shows a comparison of the predicted vertical profiles of HNO_3 at a variety of longitudes with the profiles measured by Huebert and Lazrus (1980) during the GAMETAG aircraft experiments. Panel (a) compares the model to the data taken in remote Pacific Ocean locations while panel (b) compares the model to data from North American continental locations. Huebert and Lazrus used a chemical reaction to convert HNO_3 vapor in air to a nonvolatile nitrate salt; this means that all acidic nitrogenous gases contribute to the measured concentration. It is therefore possible that in addition to the vapor-phase nitric acid and particulate nitrate, an unspecified amount of PAN and pernitric acid was included in their measurement. The predicted values in remote areas are in reasonable agreement with the measured concentrations, but those over continental areas are somewhat high. Figure 3 displays a comparison of the same data with a latitudenal profile of

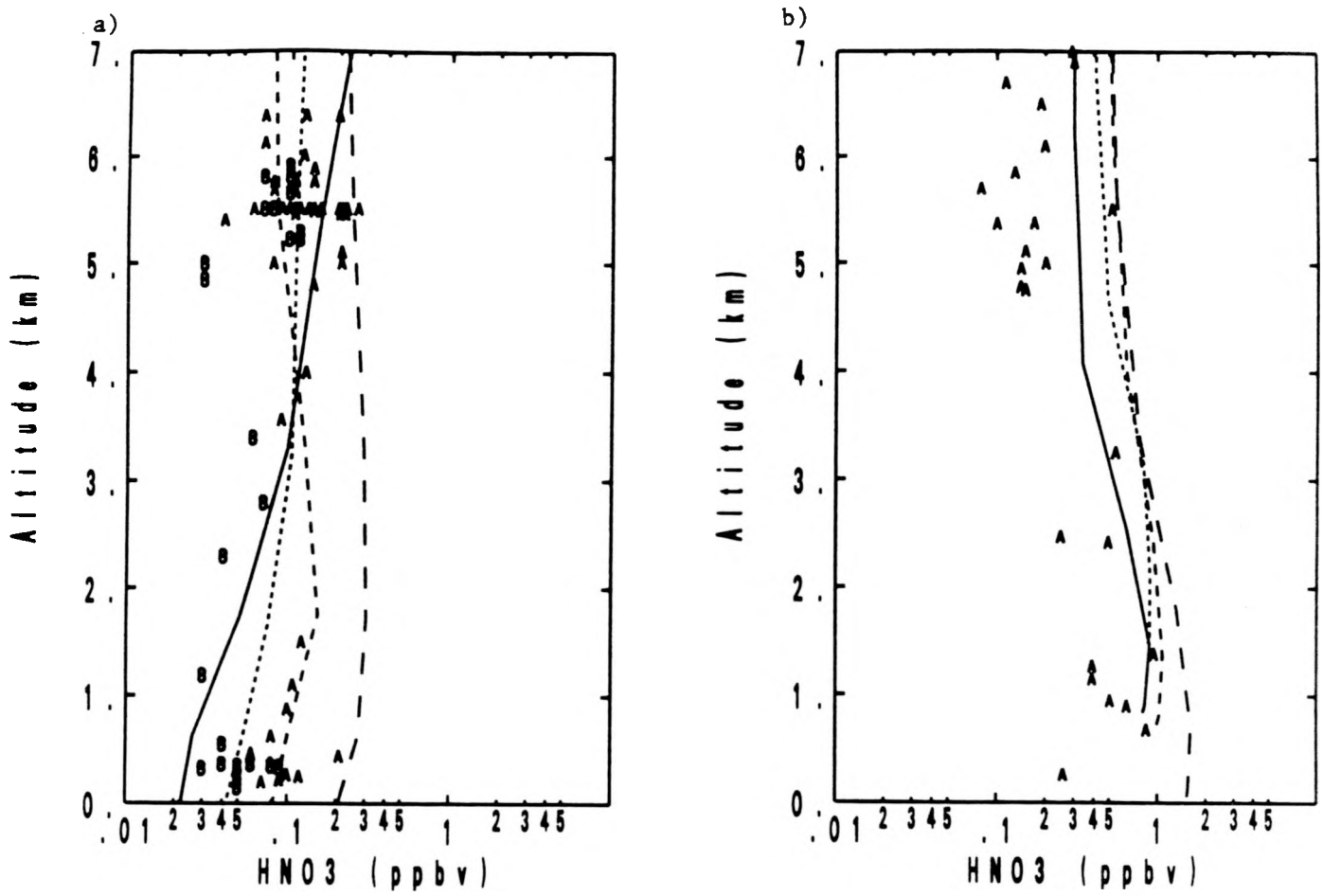

Figure 2. Vertical profiles of HNO_3 are compared with measurements of HNO_3 by Huebert and Lazrus (1980). The symbol A refers to measured mean concentrations while symbol B refers to a measured upper limit where the value of HNO_3 lies between zero and the symbol B. In panel (a) the July model results for the Pacific Ocean (125W) are compared with Huebert and Lazrus (1980) Pacific Ocean measurements. Latitudes shown are 40S (line), 20S (short dash), 0 (longer dash), and 20N (longest dash). Panel (b) shows model predictions for continental locations at 40N and 120W (line), 110W (short dash), 100W (longer dash), and 90W (longest dash) in July along with the continental North American data of Huebert and Lazrus (1980).

the predicted concentrations in the boundary layer (Figure 3a) and in the free troposphere (Figure 3b). The free tropospheric values appear to be somewhat high.

In contrast to the comparison of our predictions with the data of Huebert and Lazrus, where we tend to be somewhat high, the predicted concentrations from the model appear to be low relative to the surface concentrations of nitrate measured during the SEAREX program (Savoie et al., 1989a). Savoie et al. (1989 a,b) measured nitrate using a high-volume sampling system and their measurements refer to total inorganic nitrate (i.e., particulate nitrate plus gaseous HNO_3), but it is believed that much of the nitrate is present in the

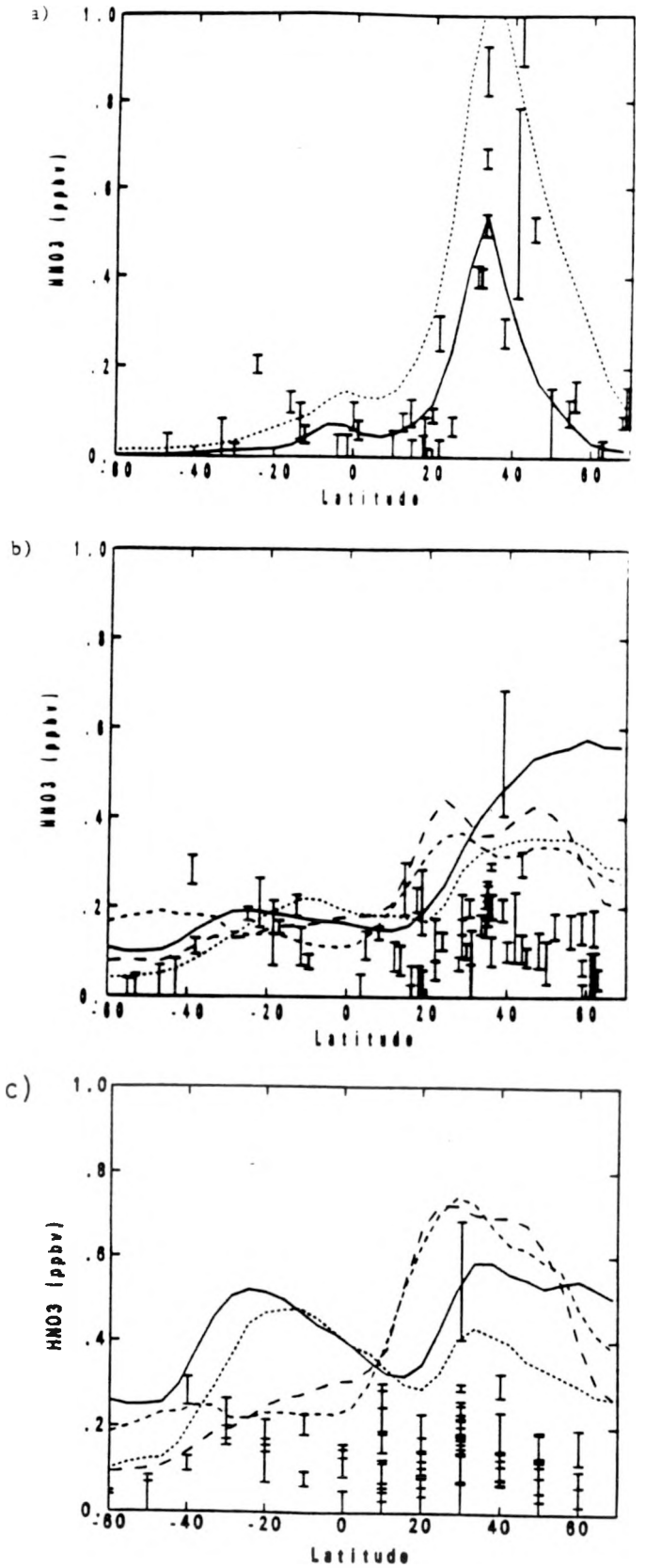

Figure 3. Predicted HNO_3 profiles for the 112.5W meridian for January and July. Also presented are the latitudinal profiles measured by Huebert and Lazrus (1980) during August and September, 1977 and May and June, 1978. Panel (a) shows model results for 991 mb using the sources specified in Table 1 along with boundary layer measurements. January and July calculations are shown by a solid line and short dashed line, respectively. Panel (b) shows model results for 500 mb and 664 mb, using the sources specified in Table 1 along with free troposphere measurements. Panel (c) shows model results for 500 mb and 664 mb with the lightning source increased from 3 Mt N/yr to 10 Mt N/yr. In panels (b) and (c), the calculations are for January, 500 mb (solid line) and 664 mb (short dash), and for July, 500 mb (longer dash), and 664 mb (longest dash), respectively.

particulate form. Figure 4 shows the average of our January and July predicted HNO_3 concentrations together with the measured concentrations at the SEAREX Pacific Island stations. Here we assume that our predicted HNO_3 vapor would be converted to particulate nitrate in this marine environment. The solid lines in this figure indicate the 95% confidence levels of the measured mean concentration. The symbols marked "A" in this figure show the predicted concentrations for the model with 3 Mt N from lightning. The symbols marked "B" show the predicted concentrations for a simulation in which the source of NO_x from lightning is increased to 10 Mt N/yr. For the latter simulation, the agreement with the data of Savoie et al. is much better. Increasing the lightning source from 3 to 10 Mt has a much larger effect on the predicted concentrations in the mid-Pacific than does a change in the surface-based soil microbial source. This is shown by symbol "C" in the figure, which considered an increase in the soil microbial source from 10 to 15 Mt N/yr. These symbols nearly overlay those from the model run with only 10 Mt N from soils.

Although the comparison of the model results with 10 Mt N from lightning to the data of Savoie et al. is much better than the comparison with only 3 Mt N, increasing this source degrades our agreement with the data of Huebert and Lazrus (1980). This is demonstrated in Figure 3c which shows a comparison between the measurements of Huebert and Lazrus (1980) and the model predicted concentrations in the free troposphere with the lightning source increased from 3 Mt N/yr to 10 Mt N/yr. For 10 Mt N, the predicted concentrations appear to be about a factor of 2 too high relative to those measured.

There are several possible explanations for these contrasting results. First, there may be a marine source of nitrate that contributes to the surface-based measurements of Savoie et al. (1989a) but is not represented in the model (note also comments of Savoie et al., 1989a). A marine source of nitrate is consistent with the observation of a nitrate component to the marine signature from the principal component analysis for arctic aerosol reported by Li and Winchester (1989). The marine nitrate source may not contribute to the free-tropospheric concentrations of nitrate measured by Huebert and Lazrus (1980) if it is removed quickly by deposition processes, for example. Second, the aircraft-based measurements of HNO_3 may be low. Aircraft-based observations of nitrate are notoriously difficult. For example, it is possible that some loss of nitrate occurs along the inlet tubes between tropospheric air and the filter samplers. Also, recent experiments have shown that different techniques can give different abundances of nitrate (Singh, private communication, 1990). Thus, further research is needed to determine whether the upper level nitrate measurements need to be revised. The third possible reason for the discrepancy between our predictions at the SEAREX sites relative to the measurements and our predictions of HNO_3 in the upper troposphere relative to the data of Huebert and Lazrus (1980) is deficiencies in the model chemistry. Thus, the model may not properly account for the contribution of PAN (peroxyacetyl nitrate) and other organic nitrates to the dispersion of reactive nitrogen from land-based sources. While it is clear that PAN is an important reactive nitrogen carrier at lower levels and perhaps throughout the troposphere in the winter hemisphere (indeed, Singh et al. (1986) measure concentrations as high as 500 ppt in many remote areas in the winter), its importance as a reactive nitrogen carrier in the summer hemisphere is apparently not yet established. Thus, measurements in the summer hemisphere, particularly those above about 4 km are reported to be only several tens of

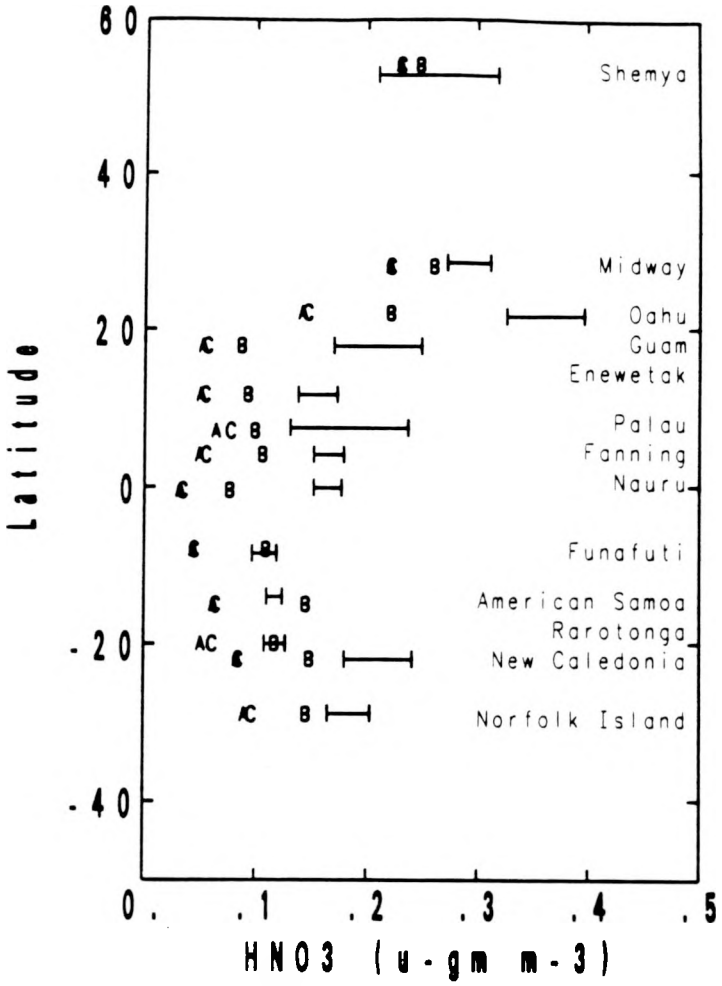

Figure 4. The mean January and July model predictions of surface HNO_3 concentrations in microgram/m^3 for various Pacific Ocean locations. Symbol A represents the standard model with sources as indicated in Table 1. Symbol B represents a model run in which the lightning source was increased from 3 to 10 Mt N/yr while symbol C represents a run in which the soil source was increased from 10 to 15 Mt N/yr. Also shown are the 95% confidence levels of the measured mean concentrations of inorganic nitrate measured by Savoie et al. (1989a).

ppt by some authors (Rudolph et al., 1987), but average values near 125 ppt as reported by others (Singh et al., 1990). Values of only a few tens of ppt would be close to our predicted NO_x concentrations at upper altitudes over coastal and mid-ocean locations, but values of over 100 ppt would be several times larger. The latter concentration, if present over large regions of the upper troposphere, would indicate that PAN should be considered as an important carrier of reactive nitrogen even in the summer hemisphere and might explain why our predictions are high relative to the upper-air measurements of Huebert and Lazrus (1980) but low relative to the boundary layer measurements of Savoie et al. (1989 a,b). Further research and measurements should clarify which of the above three explanations is most plausible.

4. Geographical and Seasonal Distribution of HNO_3 and NO_x and the Role of Anthropogenic Sources

Figures 5a and 5b show the predicted NO_x surface concentrations for January and July with all sources represented in the model. In January, the surface concentrations of NO_x over Eastern North America and Europe reach values as high as 4 ppb. In July, the maximum surface concentration contours are only 1 and 2 ppb, respectively. The smaller concentrations in July are the result of higher concentrations of OH in the summer hemisphere. This acts to convert NO_x to HNO_3 more quickly. Also to be noticed are the relatively large concentrations of NO_x over South America, Africa, and Asia. These result from a combination of biomass burning and soil microbial sources in the tropics and fossil fuel and soil sources in Asia.

5. Global Deposition

Wet Deposition

Maps of wet deposition of HNO_3 in both January and July are shown for the all sources scenario in Figure 6. Wet deposition is expressed as kg N km^{-2} deposited for the entire month (either January or July).

The wet deposition of HNO_3 due to all sources is shown in Figure 6a for January. The peak continental wet HNO_3 deposition magnitudes are comparable for many regions. For example, South America and southern Africa are both enveloped by the 3 kg N km^{-2} contour, and have peak contours of 15 kg N km^{-2}. Likewise, in the Northern Hemisphere the 3 kg N km^{-2} contour encircles the eastern U.S., much of Europe, and a region from east Asia across the North Pacific Ocean. Peak values are 15, 5, and 10 kg N km^{-2} for the U.S., Europe, and east Asia, respectively. Additionally, a 1 kg N km^{-2} contour covers most of the oceans north of 20° S.

Although the precipitation in the Northern and Southern Hemispheres contains comparable HNO_3 levels, different sources are responsible. In Figure 6a, the deposition pattern in the Northern Hemisphere is fairly similar to that for fossil fuel sources. Elsewhere, the peaks in South America and Africa in Figure 6a resemble, but are larger than those for natural sources only. All sources include biomass burning, the geographical distribution of which resembles that of soil emissions in the tropical regions. The biomass burning source is greatest in January over the Southern Hemisphere continents of South America, Africa, and Australia.

The total wet HNO_3 deposition for all sources in July is given in Figure 6b. Nitric acid levels in precipitation are comparable for the Southern Hemisphere (South America and Africa) and Northern Hemisphere (North America, Europe, and east Asia) regions, but for different reasons. The peaks over South America and Africa shift northwards in July, as does the precipitation pattern (Pitcher et al., 1983).

Conclusions about wet HNO_3 deposition on a regional basis also hold on a hemispheric scale because within each hemisphere most regions have similar fuel use and vegetation patterns. The January and July wet HNO_3 deposition patterns in Table 3 reflect this. In the Northern Hemisphere, fossil fuel sources account for roughly 51–53% of wet HNO_3

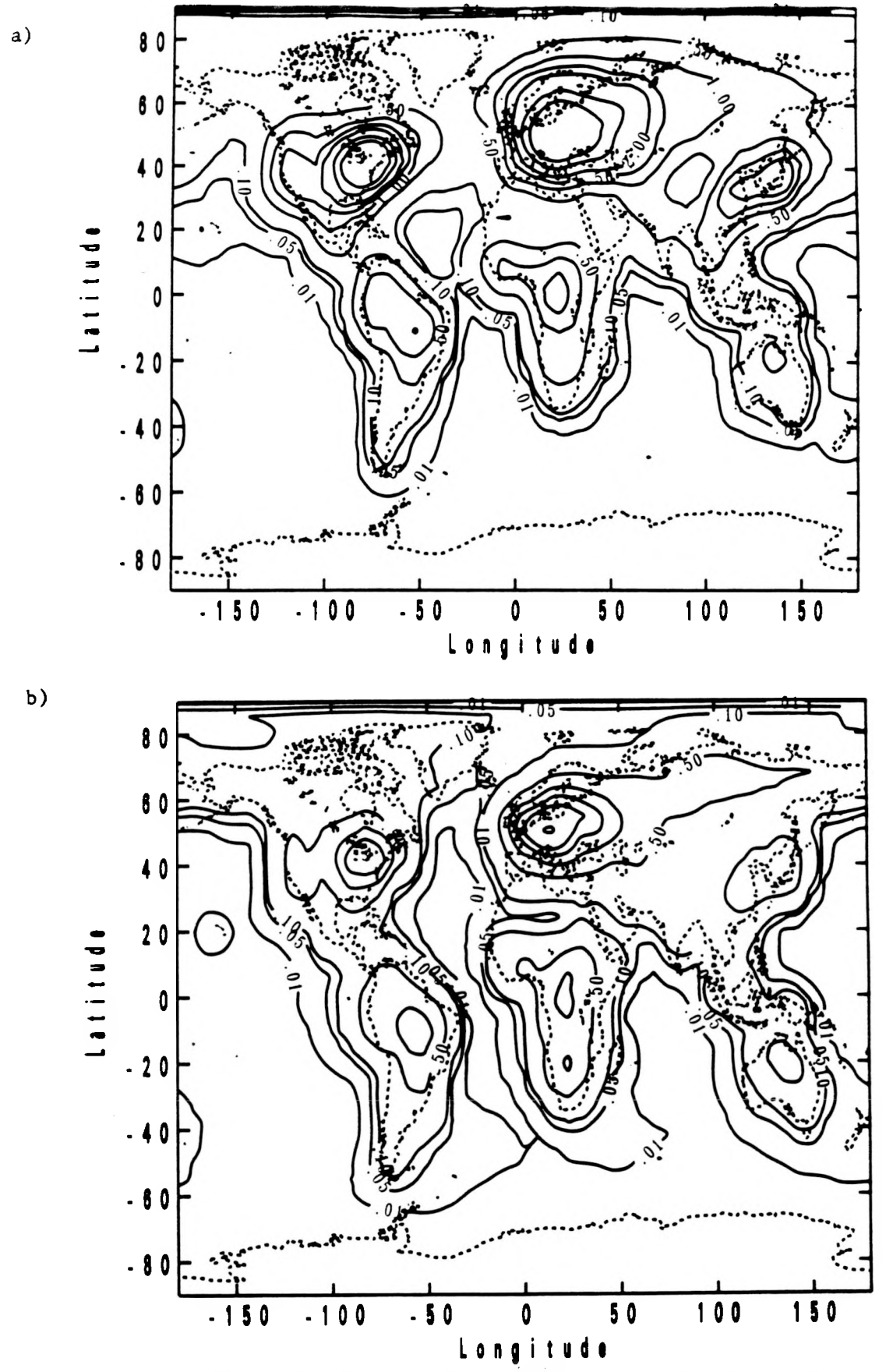

Figure 5. Model calculated distributions of NO_x surface mixing ratios for (a) January and (b) July in ppbv when all sources listed in Table 1 are considered. Contour intervals are 0.01, 0.05, 0.1, 0.5, 1.0, 1.5, 2.0, 3.0, and 4.0 ppbv.

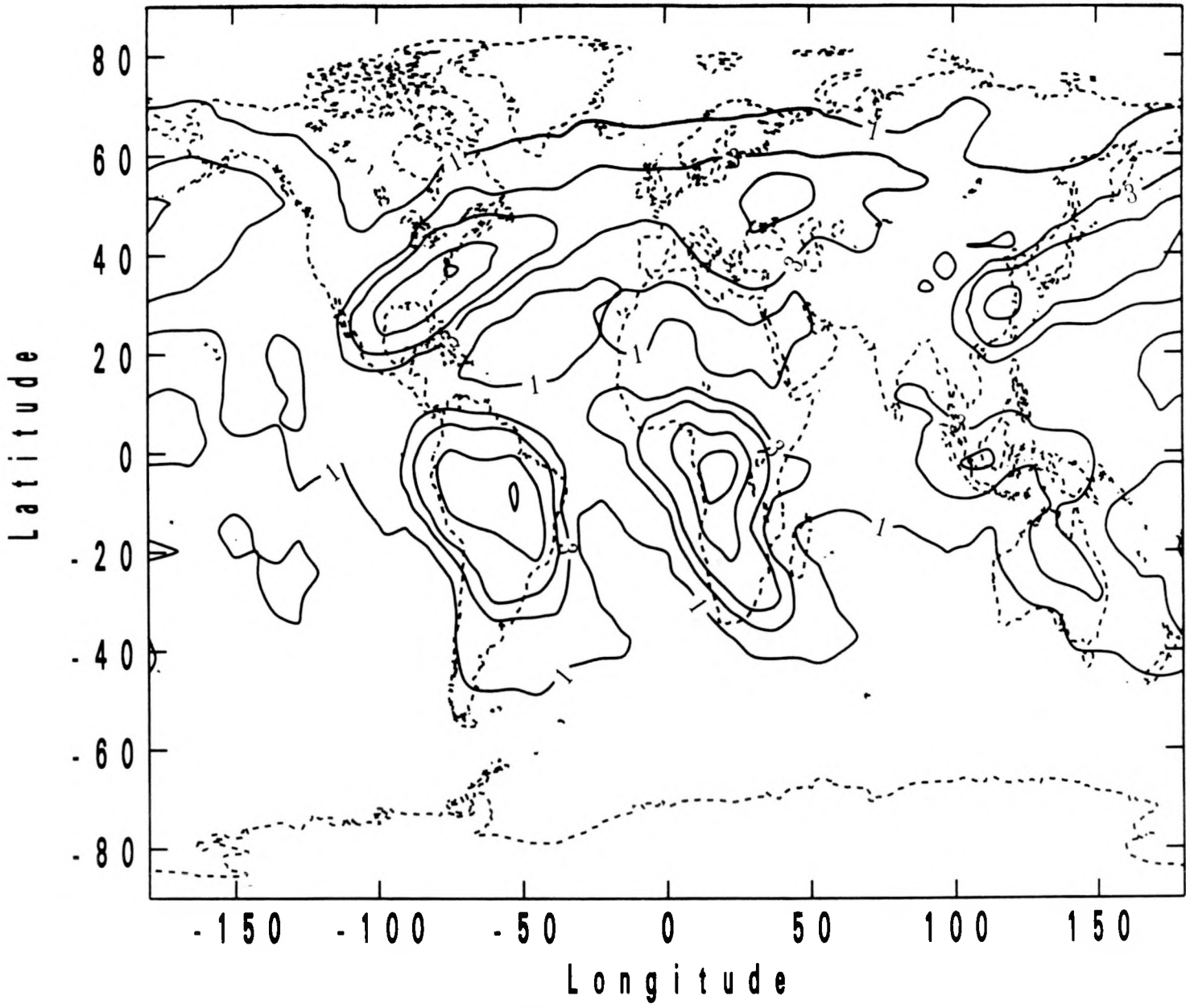

Figure 6a. The mass of HNO_3 removed by precipitation in January, when all sources of NO_x are considered, in units of kg N km^{-2}. Contour intervals are 1, 3, 5, 10, 15, 20, 30, and 40 kg N km^{-2}.

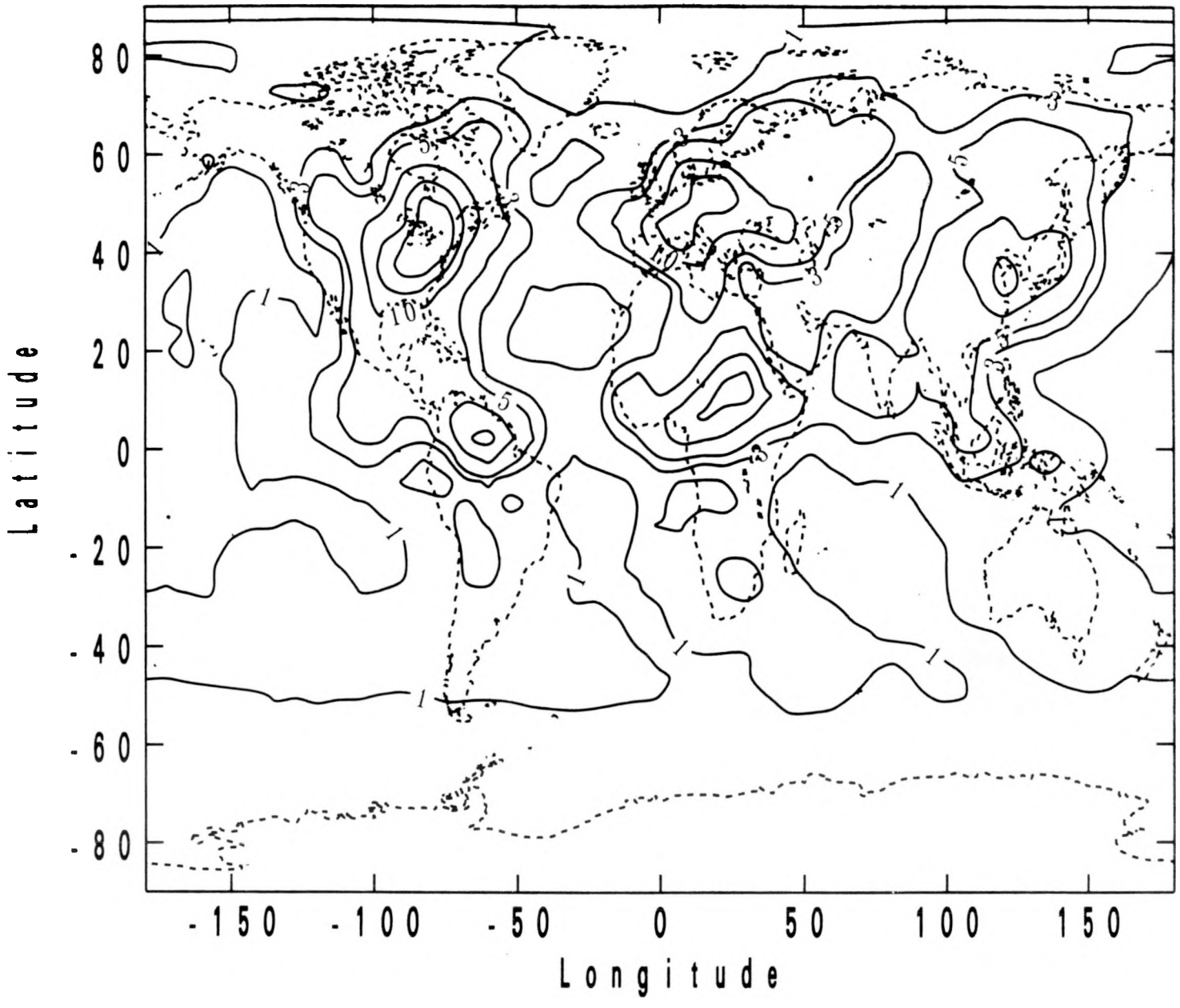

Figure 6b. The mass of HNO_3 removed by precipitation in July when all sources of NO_x are considered, in units of kg N km^{-2}. Contour intervals are 1, 3, 5, 10, 15, 20, 30, and 40 kg N km^{-2}.

deposition and natural sources for 34–38%. (By far the largest natural source in July for the Northern Hemisphere is soil emissions.) In the Southern Hemisphere, 60–63% of the wet HNO_3 in precipitation arises from natural sources. The biomass burning source is as large as the soil emission source in January and is the second largest source in July. Fossil fuel sources rank third and account for only 11–12% of the wet HNO_3 deposition.

Table 3. Wet HNO_3 deposition for three different scenarios in units of kg N month^{-1}.

	J A N U A R Y		J U L Y	
Scenario	Northern Hemisphere	Southern Hemisphere	Northern Hemisphere	Southern Hemisphere
Fossil Fuel	3.5 (8)	4.4 (7)	6.3 (8)	3.2 (7)
Natural	2.6 (8)	2.5 (8)	4.1 (8)	1.7 (8)
All Sources	6.9 (8)	4.2 (8)	1.2 (9)	2.7 (8)

On both a regional and hemispheric basis, the following conclusions can be made. First, the amount of HNO_3 removed by precipitation is predicted to be comparable for the Northern and Southern Hemisphere continents. However, very different sources of NO_x are responsible. In the Northern Hemisphere, fossil fuel sources are dominant. In July, the natural sources of mainly soil emissions, but some lightning, contribute also. Conversely, in January, the dominant NO_x sources in the Southern Hemisphere are soil emissions and biomass burning. In July, the dominant Southern Hemisphere source is soil emissions, followed by biomass burning. In both January and July, the fossil fuel combustion source is only third in magnitude in the Southern Hemisphere.

Dry Deposition

Dry deposition is an important process for the reactive nitrogen cycle. Logan (1983) estimated global loss rates of nitrate to be 12–22 Tg N yr^{-1} by dry deposition and 12–42 Tg N yr^{-1} by wet deposition. Based on field measurements, Huebert and Robert (1985) estimated a dry deposition flux of 24.4–31.1 kg N km^{-2} for gaseous HNO_3 in the month of June in an Illinois pasture. For that same month, the nearby National Acid Deposition Program (NADP) site recorded a wet-nitrate deposition rate of 33.9 kg N km^{-2}. Thus, wet and dry deposition of HNO_3 were comparable in magnitude.

Table 4 presents dry and wet deposition amounts for the two hemispheres for January and July. Consider first the Southern Hemisphere. In January (summer), higher photolysis rates mean more NO_x is converted to HNO_3, and wet and dry HNO_3 deposition amounts are much greater than the amount of NO_x dry deposited. In January, dry NO_x deposition is 1.5×10^8 kg N month^{-1} (18% of the total), dry HNO_3 deposition is 2.8×10^8 kg N month^{-1} (33% of total), and wet HNO_3 deposition is 4.2×10^8 kg N month^{-1} (49% of total). Total

nitrogen deposition is 8.5×10^8 kg N month^{-1}. The situation changes for the Southern Hemisphere in July (winter). First, total deposition decreases from 8.5×10^8 kg N month^{-1} in January to 8.0×10^8 kg N month^{-1} in July. This drop occurs because in July, less HNO_3 is formed and wet deposited. However, although wet deposition of HNO_3 decreases, its dry deposition increases. This is due, in part, to the northward shifted precipitation patterns, which lead to less wet HNO_3 deposition. Therefore, relatively more HNO_3 is available for dry deposition. Dry NO_x deposition increases in July to 2.1×10^8 kg N month^{-1} (26% of the total deposition) because more NO_x is present. In summary, for the Southern Hemisphere in January and July, dry NO_x deposition accounts for 18–26%, dry HNO_3 deposition for 33–40%, and wet HNO_3 deposition for 49–34% of total deposition. Thus, all these forms of deposition of nitrogen may be important.

Table 4. Dry and wet deposition of NO_x and HNO_3 for the all source scenario in units of kg N month^{-1}.

	J A N U A R Y		J U L Y	
	Northern Hemisphere	Southern Hemisphere	Northern Hemisphere	Southern Hemisphere
NO_x dry deposition	1.1 (9)	1.5 (8)	6.1 (8)	2.1 (8)
HNO_3 dry deposition	6.5 (8)	2.8 (8)	1.1 (9)	3.2 (8)
Total dry deposition	1.8 (9)	4.3 (8)	1.7 (9)	5.3 (8)
HNO_3 wet deposition	6.9 (8)	4.2 (8)	1.2 (9)	2.7 (8)
Total Wet & Dry Deposition	2.5 (9)	8.5 (8)	2.9 (9)	8.0 (8)

The Northern Hemisphere shows similar seasonal trends. In July (summer), total deposition (2.9×10^9 kg N month^{-1}) is higher than January (2.5×10^9 kg N month^{-1}) because more HNO_3 is formed in July. In July wet HNO_3 deposition (1.2×10^9 kg N month^{-1} or 41% of the total) and dry HNO_3 deposition (1.1×10^9 kg N month^{-1} or 38% of the total) are comparable. Dry NO_x deposition (6.1×10^8 kg N month^{-1}) accounts for 21% of all deposition. In January, however, NO_x dry deposition increases to 1.1×10^9 kg N month^{-1} (44% of the total deposition), HNO_3 dry deposition decreases to 6.5×10^8 kg N month^{-1} (or 26% of the total), and HNO_3 wet deposition decreases to 6.9×10^8 kg N month^{-1} (or 28% of the total). Overall, total deposition also decreases from its July value. Again, as for the Southern Hemisphere case, wet (28–41%) and dry (26–38%) HNO_3 deposition are comparable. The dry NO_x deposition is also important and can account for 44–21% of total deposition, in January and July.

In summary, the dry deposition of both HNO_3 and NO_x can be important. The dry deposition of HNO_3 is generally comparable to its wet deposition. Additionally, NO_x dry

deposition can account for 18–44% of total deposition for the Northern and Southern Hemispheres. The deposition amounts are also functions of season. The relative importance of NO_x dry deposition increases in the winter, when the conversion of NO_x to HNO_3 is slower and more NO_x is present. These calculations, of course, are based on a very simple model of dry deposition and on highly uncertain dry deposition velocities. The results may be subject to change as more information becomes available in the future.

6. Regional Analysis of Sources and Deposition

The results presented in Section 5 is summarized here by continent. This information is presented for the January and July all source scenarios in Figures 7 and 8, respectively. Emissions and deposition are graphically presented for six regions, which are defined by the following coordinates: U.S. (29° N, 128° E to 47° N, 68° E); Canada (47° N, 135° E to 64° N, 60° E); Europe (38° N, 8° E to 73° N, 30° W); China (20° N, 75° W to 51° N, 128° W); Africa (38° S, 15° E to 33° N, 38° W); and South America (56° E, 83° S to 11° N, 38° E). As discussed above, all the regions shown have the same order of magnitude of emissions, although the sources responsible vary. Thus, the dominant sources for Northern Hemisphere regions (U.S., Canada, Europe, China) are fossil fuel combustion, followed by soil emissions. Conversely, for the equatorial and Southern Hemisphere continents of South America and Africa, the primary NO_x sources are soil emissions and biomass burning.

The deposition results also reflect the findings discussed earlier for the Northern and Southern Hemispheres. All three types of deposition (dry NO_x, wet HNO_3, dry HNO_3) contribute significantly to total deposition. In January (Figure 7), the Northern Hemisphere regions see relatively strong NO_x dry deposition, due to the slow wintertime conversion of NO_x to HNO_3. Conversely, the Southern Hemisphere regions of South America and Africa, see substantial deposition (wet and dry) of HNO_3 in this summer month.

The situation differs slightly in July. Figure 8 shows the all source scenario. In the Northern Hemisphere, more NO_x is converted to HNO_3. Thus, NO_x dry deposition is low, while HNO_3 wet and dry deposition are relatively higher. For the Southern Hemisphere regions in South America and Africa in July (winter), more NO_x is present. Consequently, NO_x dry deposition is relatively larger (especially for South America, which is almost entirely contained in the Southern Hemisphere).

When these continental regions export reactive nitrogen, the oceans are also affected. Deposition over oceanic regions is addressed in Table 5. The five regions are defined as the north Atlantic (11° N, 60° W to 60° N, 15° W), south Atlantic (60° S, 30° W to 2° S, 8° E), Indian (60° S, 53° E to 11° S, 113° E), north Pacific (2° S, 150° E to 60° N, 135° W), and south Pacific (60° S, 180° to 2° S, 83° W) Oceans. Natural NO_x sources due to lightning and transport from the stratosphere are present over the oceans. Thus, deposition when all sources are considered should be compared to deposition for the natural source scenario. Table 5 for January shows that 80% of the deposition over the north Atlantic and 72% of the deposition over the north Pacific come from anthropogenic sources of nitrogen. These two regions are by far the most strongly affected oceanic regions considered. The result implies that anthropogenic activities on the North American and European/Asian continents contribute to nitrogen deposition over very large oceanic regions.

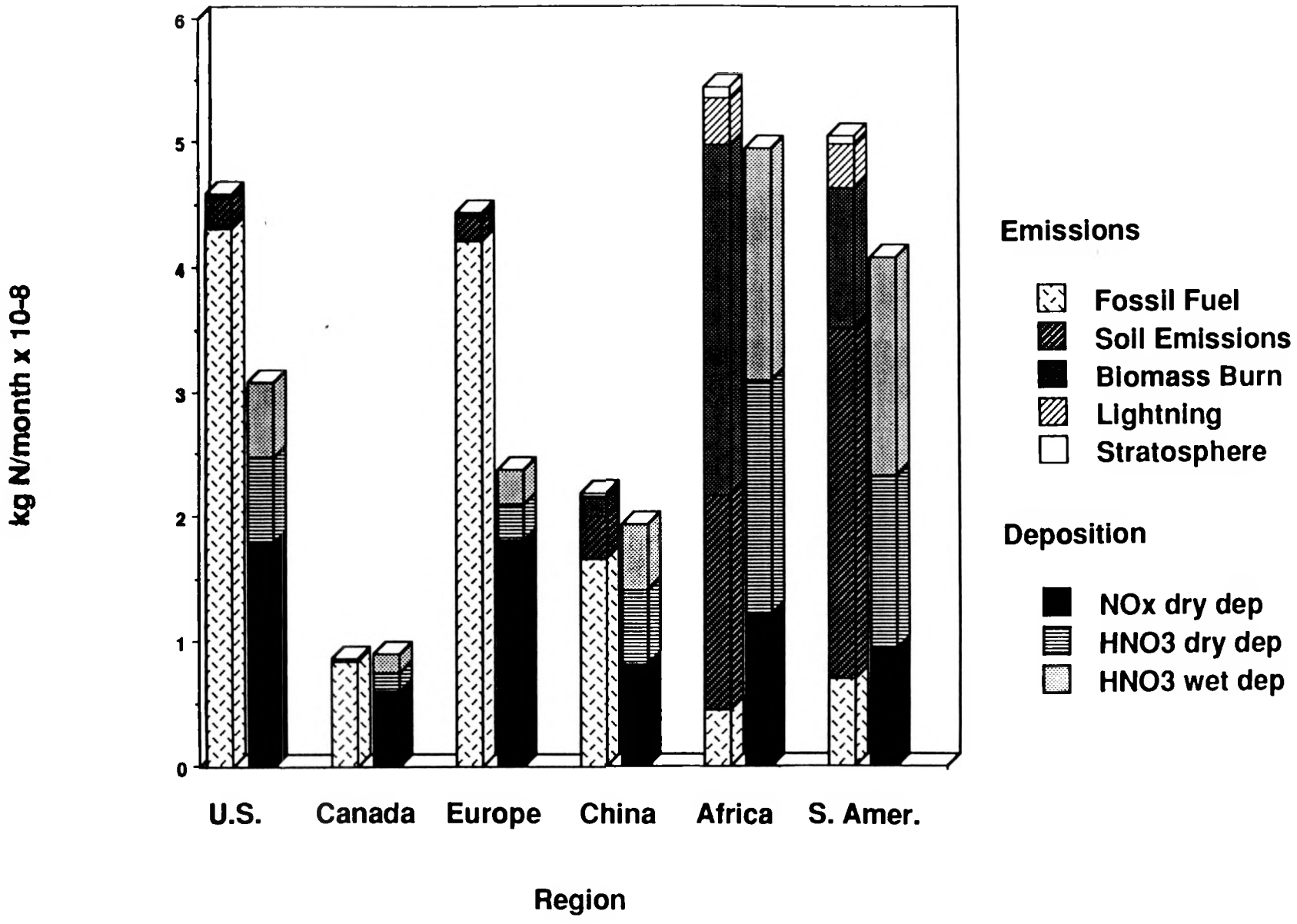

Figure 7. Regional emission and deposition amounts for January when all sources of NO_x are considered. For each region, emissions are given by the left column, and deposition by the right. For each region, sources include fossil fuel combustion, soil emissions, biomass burning, lightning, and transport from the stratosphere, and deposition is composed of NO_x dry deposition, HNO_3 dry deposition, and HNO_3 wet deposition.

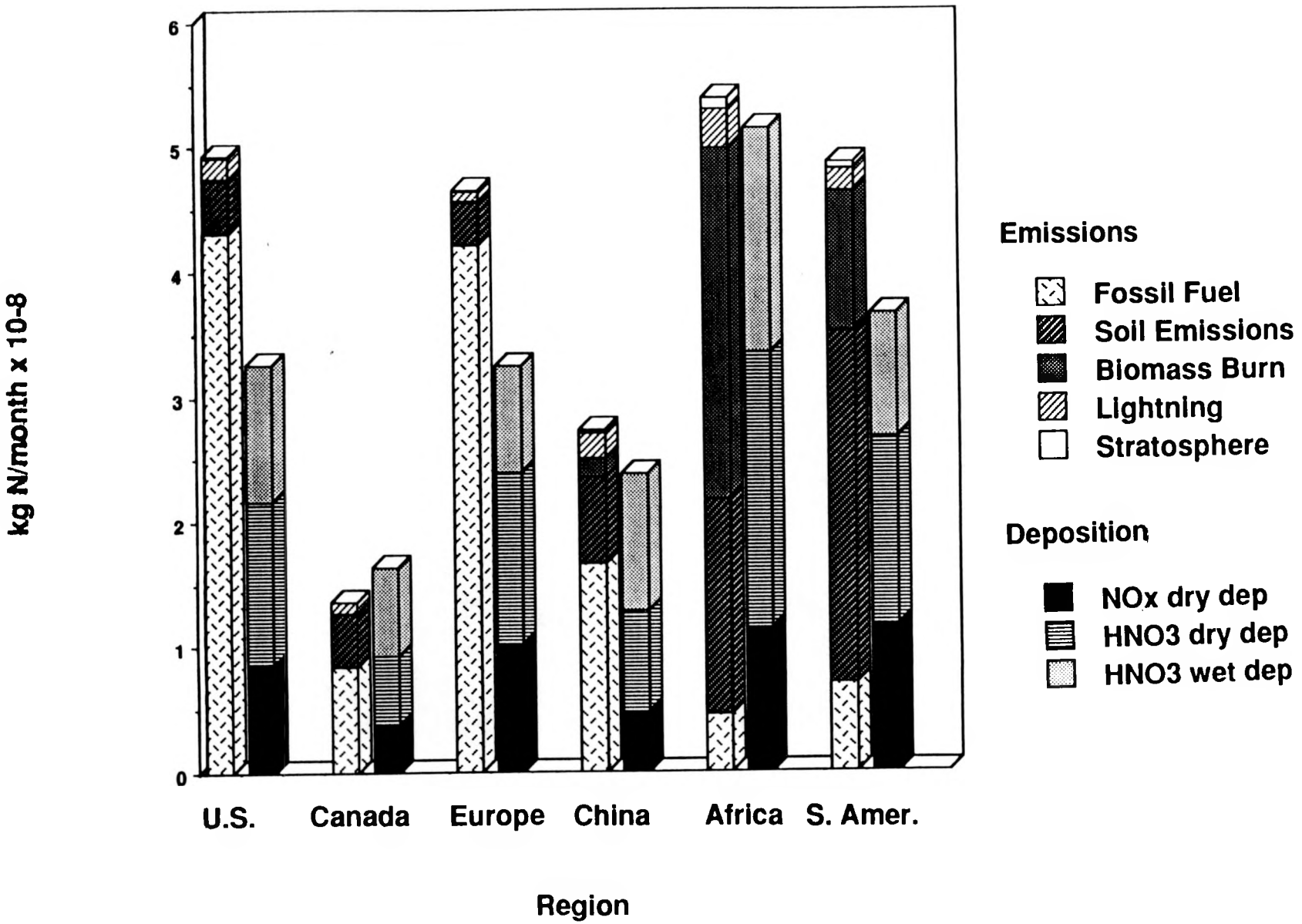

Figure 8. Regional emission and deposition amounts for July when all sources of NO_x are considered. For each region, emissions are given by the left column, and deposition by the right. For each region, sources include fossil fuel combustion, soil emissions, biomass burning, lightning, and transport from the stratosphere and deposition is composed of NO_x dry deposition, HNO_3 dry deposition, and HNO_3 wet deposition.

Table 5. Total deposition (wet and dry) of reactive nitrogen over oceanic regions, in kg N $month^{-1}$.

JANUARY	North Atlantic Ocean	South Atlantic Ocean	Indian Ocean	North Pacific Ocean	South Pacific Ocean
Natural Sources only	2.4 (7)	2.6 (7)	1.9 (7)	5.7 (7)	5.0 (7)
All Sources	1.2 (8)	4.5 (7)	2.7 (7)	2.0 (8)	6.2 (7)
% dep due to anthropogenic sources	80%	42%	30%	72%	19%
JULY					
Natural Sources Only	2.5 (7)	2.8 (7)	2.6 (7)	3.8 (7)	8.0 (7)
All Sources	8.0 (7)	5.7 (7)	4.1 (7)	8.0 (7)	1.2 (8)
% dep due to anthropogenic sources	69%	51%	37%	53%	33%

Three other oceanic regions—the south Atlantic, Indian, and south Pacific Oceans receive less total nitrogen deposition than the Northern Hemisphere oceans, and a relatively smaller fraction is due to anthropogenic nitrogen sources. This is expected because these three oceans lie in the Southern Hemisphere, where the largest nitrogen source is natural: soil emissions. However, the fraction from anthropogenic sources is still surprisingly large, ranging from 19–42%.

In July, the anthropogenic fraction of deposition over the oceans in the Northern Hemisphere drops but is still large. Thus, 69% of the total deposition for the North Atlantic is due to anthropogenic nitrogen while 53% of total deposition is anthropogenic for the north Pacific Ocean. The fraction drops in July because soil emissions and the lightning source increase in the Northern Hemisphere, leading to a stronger natural source term and a smaller anthropogenic deposition fraction. The converse holds in the Southern Hemisphere. In July (winter), natural sources (mainly lightning) decrease. Thus, the anthropogenic deposition fraction increases somewhat, from 42% to 51% for the south Atlantic, from 19 to 33% for the south Pacific, and from 30 to 37% for the Indian Ocean, from January to July.

Thus, man's activities contribute a significant fraction of the amount of oceanic nitrogen deposition. In the Northern Hemisphere, anthropogenic sources of reactive nitrogen from the burning of fossil fuel and biomass may account for 53–80% of the nitrogen deposited to oceanic surfaces. In the Southern Hemisphere, these anthropogenic sources contribute roughly 19–51% of the total nitrogen deposition to oceans.

7. Conclusions

Figure 9 shows the ratio of our predicted surface concentrations of NO_x for all sources in July to the predicted surface concentrations for natural sources only. (In this figure, the 3 Mt lightning source has been used). As shown there, vast areas of the globe have experienced increased concentrations of NO_x as a result of man's activities. These increased concentrations may have already contributed to the increased concentrations of O_3 that have been observed at many Northern Hemisphere continental sites (Angell and Korshover, 1983; Bojkov, 1986; Janach, 1989; Volz and Kley, 1988; Logan, 1985). According to our model, it appears that increases in O_3 may also be possible over large regions in the Southern Hemisphere and over the oceans.

We have also shown that precipitation in the Northern and Southern Hemispheres deposits comparable amounts of HNO_3, but for different reasons. In the Northern Hemisphere, the largest fraction of HNO_3 wet deposition is due to fossil fuel sources, followed by soil emissions in both January and July. In the Southern Hemisphere both in January and July, HNO_3 deposition in precipitation arises due equally to soil emissions of nitrogen and biomass burning, followed by fossil fuel combustion.

We have shown that we are able to successfully simulate many of the observed features of the reactive nitrogen cycle in the troposphere. Many significant problems remain to be addressed. In particular, there is a need to quantify the role of anthropogenic sources of NO_x in the global budget of O_3. The spatial extent of the contribution of anthropogenic sources of NO_x to surface concentrations is unexpected. In the future, we hope to extend our model in order to quantify the role of anthropogenic sources of NO_x in the global budget of tropospheric O_3.

8. Acknowledgements

This work was supported by the U.S. E.P.A. under Interagency Agreement DW89932676-01-0 and by the Institutional Research and Development Program of the Lawrence Livermore National Laboratory. Computer time was supplied by the D.O.E. Office of Health and Energy Research. Lawrence Livermore National Laboratory is operated by the University of California under contract number W-7405-Eng-48 with the U.S. Department of Energy.

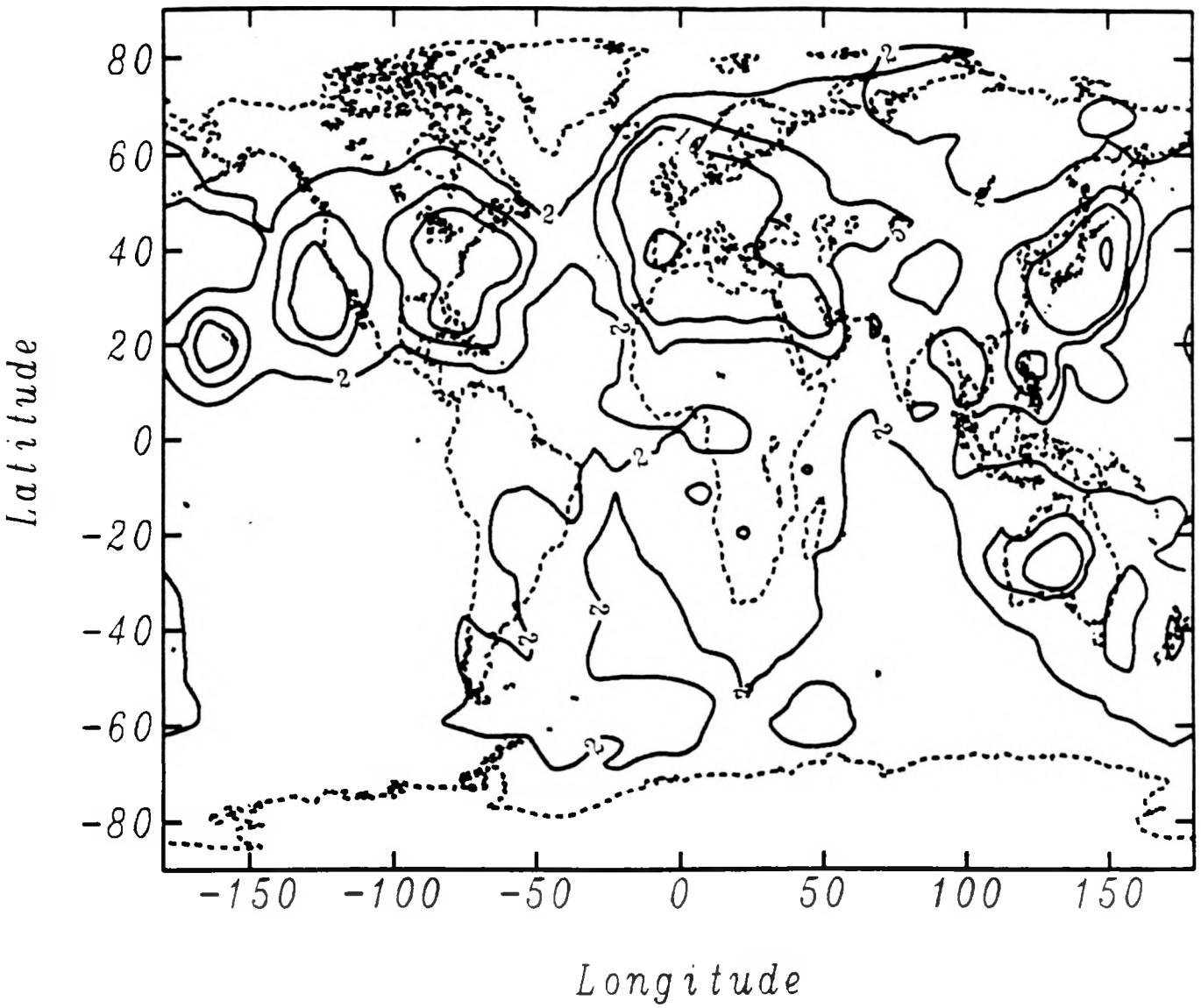

Figure 9. The ratio of the predicted surface concentrations of NO_x for all sources in July to the predicted surface concentrations for natural sources only. The calculation with natural sources only included soil microbial activity, lightning discharges, and production in the stratosphere (see Table 1). The increased concentrations in the Northern Hemisphere are mainly the result of fossil fuel burning, while both fossil fuel burning and biomass burning contribute in the tropics and Southern Hemisphere.

8. References

Angell, J.K. and J. Korshover, "Global Variation in Total Ozone and Layer-Mean Ozone: An Update Through 1981," *J. Clim. Appl. Met., 22,* 1611-1627, 1983.

Atherton, C.S., J.E. Penner, J.J. Walton, and S. Hameed, "Wet and Dry Nitrogen Deposition, Results from a Global, Three-Dimensional Chemistry-Transport-Deposition Model," submitted to *Atmos. Env.,* also Lawrence Livermore National Laboratory Report UCRL-JC-103403, March 1990.

Bojkov, R.D., "Surface Ozone During the Second Half of the Nineteenth Century," *J. Clim. Appl. Met., 25,* 343-352, 1986.

Borucki, W.J. and W.L. Chamiedes, "Lightning: Estimates of the Rates of Energy Dissipation and Nitrogen Fixation," *Rev. Geophys., 22,* 363-372, 1984.

Dayan, U., J.M. Miller, W.C. Keene, J.N. Galloway, "An Analysis of Precipitation Chemistry Data from Alaska," *Atmosph. Env., 19,* 651-657, 1985.

Finlayson-Pitts, B.J., and J.N. Pitts, Jr., *Atmospheric Chemistry: Fundamentals and Experimental Techniques,* John Wiley and Sons, New York, 1098 pp., 1986.

Hameed, S., O.G. Paidoussis, and R.W. Stewart, "Implications of Natural Sources for the Latitudinal Grandient of NO_y in the Unpolluted Troposphere," *Geophys. Res. Lett., 8,* 591-594, 1981.

Hameed, S. and J. Dignon, "Change in the Geophysical Distributions of Global Emissions of NO_x and SO_x from Fossil-Fuel Combustion Between 1966 and 1980," *Atmos. Env., 22,* 441-449, 1988.

Hao, W.M., M.H. Liu, and P.J. Crutzen, "Estimates of Annual and Regional Releases of CO_2 and Other Trace Gases to the Atmosphere from Fires in the Tropics, Based on the FAO Statistics for the Period 1975-1980," presented at the Third International Symposium on Fire Ecology, Freiburg University, Federal Republic of Germany, May 16-20, 1989; also to be published in proceedings, Springer-Verlag.

Huebert, B.J. and A.L. Lazrus, "Tropospheric Gas-Phase and Particulate Nitrate Measurements," *J. Geophys. Res., 85,* 7322-7328, 1980.

Huebert, B.J. and C.H. Robert, "The Dry Deposition of Nitric Acid to Grass," *J. Geophys. Res., 90,* 2085–2090, 1985.

Janach, W.E., "Surface Ozone: Trend Details, Seasonal Variations, and Interpretation," *J. Geophys. Res., 94,* 18,289-18,295, 1989.

Kaplan, W.A., S.C. Wofsy, M. Keller, and J.M. DaCosta, "Emission of NO and Deposition of O_3 in a Tropical Forest System," *J. Geophys. Res., 93,* 1389-1395, 1988.

Keene, W.C., Personal communication, December 1988.

Kirchoff, V. W., "Are Northern Hemisphere Tropospheric Ozone Densities Larger?," *EOS, 65,* 1984.

Knapp, W.W., V.C. Bowersox, B.I. Chevone, S.V. Krupa, J.A. Lynch, and W.W. McFee, "Precipitation Chemistry in the United States, Part 1: Summary of Ion Concentration

Variability 1979-1984," Water Resources Institute Continuum, Vol. 3, Cooperative Agreement No. 58-3159-5-41, Center for Environmental Research, 468 Hollister Hall, Cornell University, Ithaca, N.Y. 14853, 1988.

Li, S.-M. and J. Winchester, "Arctic Aerosol Sulfur with Silicon but no Aluminum: Evidence for Long Range Transport of Coal Smoke," presented at the International Conference on Global and Regional Environmental Atmsopheric Chemistry, Beijing, China, May 3-10, 1989.

Likens, G.E., W.C. Keene, J.M. Miller, and J.N. Galloway, "Chemistry of Precipitation from a Remote, Terrestrial Site in Australia," *J. Geophys. Res., 88,* 1360-1368, 1983.

Logan, J.A., M.J. Prather, S.C. Wofsy, and M.B. McElroy, "Tropospheric Chemistry: A Global Perspective," *J. Geophys. Res. 86,* 7210-7254, 1981.

Logan, J.A., "Nitrogen Oxides in the Troposphere: Global and Regional Budgets," *J. Geophys. Res., 88,* 10785–10807, 1983.

Logan, J.A., "Tropospheric Ozone: Seasonal Behavior, Trends, and Anthropogenic Influence," *J. Geophys. Res., 90,* 10,463-10,482, 1985.

Oltmans, S., "Surface Ozone Measurements in Clean Air," *J. Geophys. Res., 86,* 1174-1180, 1981.

Penner, J., "Cloud Albedo, Greenhouse Effects, Atmospheric Chemistry and Climate Change," *J. of the Air and Waste Management Assoc., 40,* 456-461, 1990.

Penner, J.E., C.S. Atherton, J. Dignon, S.J. Ghan, J.J. Walton, and S. Hameed, "Tropospheric Nitrogen: A Three-Dimensional Study of Sources, Distributions, and Deposition," submitted to *J. Geophys. Res.,* and Lawrence Livermore National Laboratory Report UCRL-102183, Rev. 1, 1990.

Pitcher, E.J., R.C. Malone, V. Ramanathan, M.L. Blackmon, K. Puri, and W. Bourke, "January and July Simulations with a Spectral General Circulation Model," *J. Atmos. Sci., 40,* 580-604, 1983.

Ramanathan, V., R.J. Cicerone, H.B. Singh, and J.T. Kiehl, "Trace Gas Trends and Their Potential Role in Climate Change," *J. Geophys. Res., 90,* 5547-5566, 1985.

Reich, P.B. and R. G. Amundson, "Ambient Levels of Ozone Reduce Net Photosynthesis in Tree and Crop Species," *Science, 230,* 566-570, 1985.

Routhier, F., R. Dennett, D.D. Davis, A. Wartburg, P. Haagenson, and A.C. Delany, "Free Tropospheric and Boundary Layer Airborne Measurements of Ozone Over the Latitude Range of 58°S to 70°N," *J. Geophys. Res., 85,* 7293-7306, 1980.

Rudolph, J., B. Vierkorn-Rudolph, and F.X. Meixner, "Large-Scale Distribution of Peroxyacetylnitrate Results From the STRATOZ III Flights," *J. Geophys. Res., 92,* 6653-6661, 1987.

Savoie, D.L., J.M. Prospero, J.T. Merrill, and M. Uematsu, "Nitrate in the Atmospheric Boundary Layer of the Tropical South Pacific: Implications Regarding Sources and Transport," *J. Atmos. Chem.,* 391-415, 1989a.

Savoie, D.L., J.M. Prospero, and E.S. Saltzman, "Nitrate, Non-Seasalt Sulfate and Methanesulfonate over the Pacific Ocean," *Chemical Oceanography, 10,* 220-249, 1989b.

Singh, H.B., L.J. Salas, and W. Viezee, "Global Distribution of Peroxyacetyl Nitrate," *Nature, 321,* 588-591, 1986.

Singh, H.B., D. O'Hara, E. Condon, J. Vedder, B.A. Ridley, B.W. Gandrud, J.D. Shetter, L.J. Salas, B. Huebert, G. Hubler, M.A. Carroll, D.L. Albritton, D.D. Davis, J.D. Bradshaw, S.T. Sandholm, M. O. Rodgers, S.M.Beck, G.L. Gregory, P.J. LeBel, and J.M. Hoell, "PAN Measurements during CITE-2: Atmospheric Distribution and Precursor Relationships", in press, *J. Geophys. Res.,* May, 1990.

Sperber, K.R. and S. Hameed, "Rate of Precipitation Scavenging of Nitrates on Central Long Island," *J. Geophys. Res., 91,* 11,833-11,839, 1986.

Tilton, B.E., "Health Effects of Tropospheric Ozone," *Environ. Sci. Technol., 23,* 257-263, 1989.

Volz A. and D. Kley, "Evaluation of the Montsouris Series of Ozone Measurements Made in the Nineteenth Century," *Nature, 332,* 240-242, 1988.

Walton, J.J., M.C. MacCracken, and S.J. Ghan, "A Global-Scale Lagrangian Trace Species Model of Transport, Transformation and Removal Processes," *J. Geophys. Res., 93,* 8339-8354, 1988.

Wilcox, R.W. and A.D. Belmont, "Ozone Concentration by Latitude, Altitude and Month Near 80°W," Rep. FAS-AEQ-77-13, U.S. Dept. of Trans., Washington, D.C., 1977.

Williams, E.J., D.D. Parrish, and F.C. Fehsenfeld, "Determination of Nitrogen Oxide Emissions from Soils: Results from a Grassland Site in Colorado, United States," *J. Geophys. Res., 92,* 2173-2180, 1987.

Williamson, D.L., "Description of NCAR Community Climate Model (CCMOB),", NCAR Tech. Note, NCAR/TN-210+STR, National Center for Atmosheric Research, Boulder, CO, 1983.

WMO, *Atmospheric Ozone 1985,* Global Ozone Research and Monitoring Project, Report No. 16, NASA, Washington, D.C., USA, 1985.

Wuebbles, D.J., P.S. Connell, K.E. Grant, R. Tarp, and K.E. Taylor, "Initial Results with the LLNL 2-D Chemical-Radiative-Transport Model of the Troposphere and Stratosphere," LLNL Internal Report UCID-21178, September 1987.